8th International Symposium on Magnetic Bearing
August 26-28, 2002, Mito, Japan

A SIMPLE METHOD FOR ROTATION ABOUT THE INERTIAL AXIS OF A RIGID AMB ROTOR

Lichuan Li
Tadahiko Shinshi
Xiaoyou Zhang
Akira Shimokohbe
Precision and Intelligence Lab., Tokyo Institute of Technology, Yokohama, 226-8503 Japan
lcli@nano.pi.titech.ac.jp
shinshi@pi.titech.ac.jp
zhangxy44@pi.titech.ac.jp
shimo@pi.titech.ac.jp

ABSTRACT
In order to remove the vibration due to rotor imbalance, many methods for achieving a clean current that is free from rotational harmonics have been developed. But a clean current is known not to give the rotation about the inertial axis. In the existing methods for rotation about the inertial axis, apart from a clean current additional control has to be used and sometimes a variable rotor speed is needed, which greatly increases the complexity. In this paper we give a simple method. We use a typical clean-current technique plus a local static feedback from displacement to current. There is no need of a variable speed. Once the inertial axis is located the compensation signals can be frozen as a static function of rotor angular displacement. Then the rotation remains to be about the inertial axis for any (and also varying) rotational speed. Experiment results are included.

INTRODUCTION
It is not difficult to make a rotor at such a precision that it can be viewed as geometrically perfect. But it usually turns out to have an obvious imbalance, which causes vibration while it rotates. In applications where precise rotation about the geometric axis is not critical, the vibration can be reduced or removed by real-time control that makes rotation be about the inertial axis.

A popular approach is to maintain a clean current: to remove the synchronous component from the current by explicit canceling signal, or to prevent the current from carrying the synchronous component by controller gain design. There have been many studies (see [1]-[12], to name only a few) using various techniques including notch filters, real-time identification, adaptive control, disturbance observers, and periodic leaning. However, with a clean control current the resultant rotation is in general not about the inertial axis [1][7]. Position of the rotational axis on rotor is dependent on rotational speed. The vibration is reduced, not removed. Effectiveness is guaranteed by large air gap and small bias current [11].

The best solution is to rotate about the inertial axis, but the control will be much more complicated than to simply maintain a clean current. In [7], rotation about the inertial axis is achieved based on on-line estimation of rotor imbalance. Another case involves the use of a double notch filter and adaptive control [12], where a variable rotational speed is needed for convergence. In these cases the control is complicated, which poses a trade-off to the designer: to use the simple clean-current strategy and tolerate the remaining vibration, or to use more advanced control and enjoy complete removal of vibration. In this paper, we present a new method for rotation about the inertial axis. It is only slightly more complicated than clean-current strategy. Thus complete removal of the vibration will be more attractive.

MODELING AND STABILIZATION
Consider a rigid planar rotor with a radial AMB as shown in Figure 1, where the X-Y plane is horizontal. The planar case simplifies the development and allows attention to be concentrated on the fundamentals. It will be seen that extension to full AMBs is straightforward. The coupling between the X and Y axes is omitted and only one axis is treated whenever possible. The AMB uses the standard current control configuration. A bias current is maintained in each electromagnet. For each motion axis, a control current input is superposed with opposite signs upon the two bias currents.

When we try to let the rotor rotate about the mass center we should have a model in which the mass center is explicit. It is popular to view the geometric center as the basis and to describe the moving mass center by an imbalance force. Then the mass center is made explicit by coordinate transform. In this paper, we view the rotor as having a profile error with respect to its mass center,

and use the mass center as the basis for writing motion equations. This is natural and realistic. In fact, the rotor experiences magnetic forces only. By a torque the rotor tries to rotate about its mass center. It is essentially the profile error with respect to the mass center that causes fluctuations in air gap lengths while rotating, which then develops fluctuating magnetic forces and vibrations.

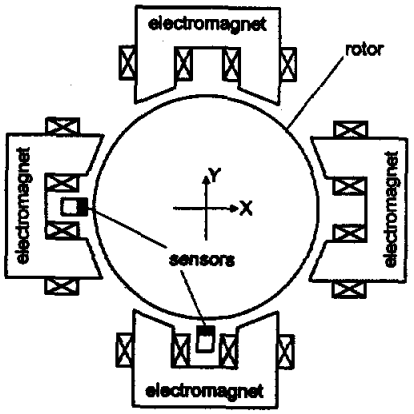

FIGURE 1: A planar rotor and AMB.

Suppose the AMB is geometrically perfect and the origin of the X-Y coordinate is at the bearing center. Any displacement is relative to this origin. Consider the motion of the rotor mass in one axis. Let x_c be the displacement of the mass center, then we have

$$m\ddot{x}_c = f \tag{1}$$

where m is rotor mass and f is the magnetic bearing force in the axis. The first-order approximation of f is known as a linear function of rotor displacement x and control current i, which gives

$$f = px + qi \tag{2}$$

where $p > 0$, $q > 0$ are constant parameters determined by the AMB geometry and the bias current. Note that x is the geometric center of the rotor. It is related to x_c by

$$x = x_c + w \tag{3}$$

where w can be viewed as rotor error with respect to x_c and is given by

$$w = a\cos\Omega t + b\sin\Omega t = A\cos(\Omega t + \varphi_0) \tag{4}$$

where a, b, A and φ are constant numbers ($a = A\cos\varphi_0$, $b = -A\sin\varphi_0$) and Ω is rotational speed in rad/s. Finally, let the control current i be related to x as following (using a displacement sensor)

$$i = i_c - kx = C(s)(r - x) - kx \tag{5}$$

where $C(s)$ is a controller for stabilization and dynamic performance, r is a reference input, $k > 0$ is a feedback gain, and $i_c = C(s)(r - x)$ is controller output. It is this k-feedback that simplifies the location of the mass center (see next section). The relationships (1)-(5) can also be represented by the block diagram in Figure 2. Note that when w is moved backward across the double integrator it becomes the familiar imbalance force, but x_c ceases to be the mass center.

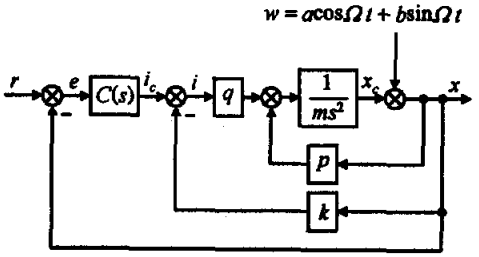

FIGURE 2: Model of rotor error.

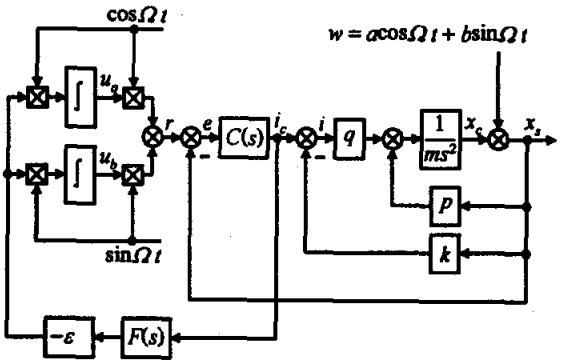

FIGURE 3: Design of compensation.

CONTROL DESIGN

In this section, we give a compensation for removing the base rotational harmonic from the controller output i_c. Then we show if $k = p/q$ the compensation leads to the rotation about the mass center. A compensation as shown in Figure 3 is designed, where square boxes with a diagonal cross denote multiplication, $\varepsilon > 0$ is constant and also small such that the stabilization dynamics is not obviously altered, and $F(s)$ is a filter. This is a SISO case of the design in [6], but the strategy for stability is different. Here we use $F(s)$ to maintain correct phase shift such that the compensation loop is stable. Let $G(s)$ be the transfer function from r to i_c, then a property of stability is stated as following. At a constant rotational speed Ω, if $F(s)G(s)$ does not have poles and zeros at $\pm j\Omega$ and its phase shift satisfies

$$|\angle F(j\omega)G(j\omega)| < \pi/2, \quad \omega \in [\Omega/a, a\Omega] \tag{6}$$

for some $a > 1$, then, for sufficiently small ε, u_a and u_b converge to some constant values such that i_c is clean. The dynamics from i_c to r (the compensation part itself) is described by a transfer function [6], with which the claim can be proved [12].

Compared to the approach in [6], where correct phase shift for convergence at different rotor speed is assured by switching parameter values in a stored lookup table, the design in Figure 3 is more easily implemented. The filter $F(s)$ does not need to be the inverse of $G(s)$. Since in our method the mass center is located at a single rotor speed, we only need to find a stable $F(s)$ satisfying (6) at the speed at which the mass center is located.

When $k = 0$ the compensation in Figure 3 is just for clean-current, and in steady-state we have $i \equiv i_c \equiv 0$. The mass center x_c is not identically zero, which is caused by w and the magnetic stiffness p. Our simple method is to cancel the effect of p by letting k be equal to an estimate of p/q. Note that to estimate this ratio is easier than to estimate either p or q. If k is exactly equal to p/q and $i_c \equiv 0$, then it follows from (1)-(3) and (5) that

$$m\ddot{x}_c = p(x_c + w) + q(i_c - kx) = qi_c = 0 \qquad (7)$$

As the stabilizing controller $C(s)$ is present, the steady-state value of x_c is zero and rotation will be about the mass center. Besides, with $k = p/q$, $i_c \equiv 0$ is achieved by a unique and rotating-speed-independent compensation signal $r = w$. Thus the location of the mass center can be identified from the converged values of u_a and u_b.

As we cannot expect k to be exactly equal to p/q, we discuss this case in more detail. Let $p - qk = h \neq 0$. Then, upon the establishment of $i_c \equiv 0$, x_c is given by

$$x_c = \frac{-h}{m\Omega^2 + h} A\cos(\Omega t + \varphi_0) \qquad (8)$$

Note that the amplitude of x_c is the error in locating the mass center. If we use the clean-current strategy ($k = 0$), upon the establishment of $i_c \equiv 0$ we should have

$$x_c = \frac{-p}{m\Omega^2 + p} A\cos(\Omega t + \varphi_0) \qquad (9)$$

Let A_k and A_0 be the amplitude of x_c given by (8) and (9), respectively. It is meaningful to compare A_k and A_0. Their ratio is

$$\frac{A_k}{A_0} = \frac{h(m\Omega^2 + p)}{p(m\Omega^2 + h)} \qquad (10)$$

It is seen that unless k is exactly equal to p/q there will be little difference between A_k and A_0 when Ω is small. For typical AMBs, p is on the order of 10^5 N/m and m is on the order of 1 kg, while h can easily be on the order of 10^4 N/m ($h/p = 0.1$). With these data, A_k/A_0 is found to be close to h/p when Ω is on the order of 10^3 rpm. This is to say that the advantage of the given method over the plain clean-current strategy can be obvious at a moderate rotational speed even if the exact value of k is not available. Note that in both (8) and (9) the amplitude of x_c approaches zero at increasing Ω, but the amplitude of acceleration d^2x_c/dt^2 does not. The ratio of maximum acceleration is also given by (10).

Another problem we should consider is associated with a minus value of h, which gives rise to a pair of zeros at $\pm j(-h/m)^{1/2}$ in $G(s)$. One choice for avoiding this problem is to use a value of k that is slightly smaller than the estimate and to tolerate a small percentage of vibration force. Another is to start the compensation in Figure 3 (by switching ε from zero to normal) when Ω is beyond the critical speed, which is $(60/2\pi)(-h/m)^{1/2}$ rpm. From the typical data used above, the critical speed is 950 rpm, which is not high. After the compensation has converged, the integrator outputs u_a and u_b can be frozen by switching ε to zero, by which the problem is avoided and the rotation remains to be about the mass center for any (and varying) rotational speed as long as the cosine and sine functions are synchronized with rotor angular position.

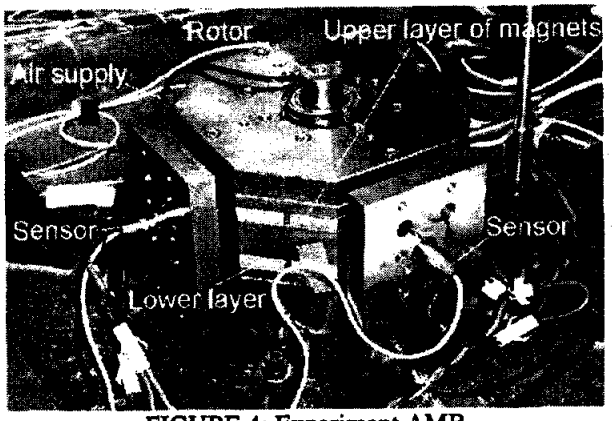

FIGURE 4: Experiment AMB

EXPERIMENT

Experiment Setup

The AMB we use for experiment is exactly the planar case we have discussed. The rotor axis is vertical. It is supported by aerostatic thrust bearings, which also keep the rotor axis from tilting. Rotor horizontal translational motion is controlled by a single radial AMB. The AMB is composed of two identical layers of electromagnets. In each layer there are four magnets configured as a standard AMB. Each electromagnet in the upper layer is connected in series with its lower counterpart, giving

four independent electromagnets. This two-layer design is to align both magnetic forces and sensors with the mass center of the rotor. The sensor and magnet targets on rotor have a common diameter of 80 mm. The sensor target has a roundness error of 30 nm, which is obtained on a Taylor Hobson measurement machine. The rotor has a disc of 158 identical and equidistant teeth. This disc is used as an air turbine for rotation. It is also used to give 158 pulses per revolution (through a sensor and some electronics), which provides information of rotor angular displacement. The assembled AMB is shown in Figure 4. The material in which magnetic flux goes is Fe-Ni sheet of 0.2-mm thickness. With the geometric parameters of the AMB and the bias current we use, the values of p and q are calculated, giving $p = 3.5\times10^5$ N/m and $q = 23.6$ N/A. The rotor mass is $m = 3.3$ kg. Rotor displacement in the X and Y axis is measured by two capacitive sensors (product of ADE, Model 5502 probe, 250 μm range, rms noise 2.7 nm, 20 kHz bandwidth). Four linear amplifiers are used, which are reshaped by local current loops of 2500 Hz bandwidth. Control is implemented on a dSPACE DS1103 board. It has CPU and supports multitasking. The sample rate we use is 10 kHz. For each sample, four repeated data (each takes 5 μs, including a 16-bit A/D conversion) of sensor output are taken, and the average is used as sensor output.

Angular Displacement Signal

The signal of 158 digital pulses per revolution triggers a subroutine. The subroutine maintains an integer output Φ that is increased by one each time it is triggered. The signal Φ is then smoothed as follows to give an angular displacement φ of the rotor

$$\varphi(s) = \frac{3c^2 s + c^3}{s^3 + 3cs^2 + 3c^2 s + c^3}\frac{2\pi\Phi(s)}{158} \qquad (11)$$

Note that there is no steady-state error in φ at constant rotor speed. With this smoothed φ the cosine and sine functions in Figure 3 can be computed meaningfully at each sample instant as $\cos\varphi$ and $\sin\varphi$. The value of c we use is $2\pi\times10$.

Controller and Parameters

In designing $C(s)$ we let $k = 0$. Later k will be identified and the feedback will be effective, which can be verified to have little influence on the stabilizing loop. $C(s)$ is

$$C(s) = \frac{B_2 s^2 + B_1 s + B_0}{s^2 + A_1 s} \qquad (12)$$

The parameters are determined by pole placement. The four closed-loop poles are all placed at $\omega_c = -2\pi\times200$. With plant parameter values, the controller parameters are calculated, yielding $B_2 = 1.34\times10^6$, $B_1 = 1.18\times10^9$, $B_0 = 3.49\times10^{11}$, and $A_1 = 5.03\times10^3$. The closed-loop transfer function $G(s)$ from r to i is found to be

$$G(s) = \frac{i(s)}{r(s)} = \frac{(ms^2 - p)(B_2 s^2 + B_1 s + B_0)}{m(s - \omega_c)^4} \qquad (13)$$

It can be checked by the parameter values that for the rotational frequencies up to 100 Hz the phase shift of $G(s)$ is close to π radians. This is true even if $k = p/q$. Thus $F(s) = -1$ guarantees the satisfaction of (6) when Ω is not high and when k is either zero or equal to p/q. For ε we choose the absolute value of the inverse of the DC gain of $G(s)$, thus $\varepsilon = m\omega_c^4/pB_0 = 6.7\times10^{-5}$.

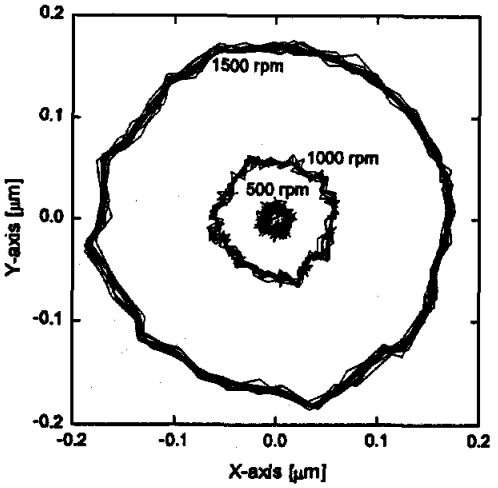

FIGURE 5: Vibration when no compensation applied.

Test without Compensation

The X and Y axes are controlled independently using two identical $C(s)$. The rotor is stabilized by $C(s)$. With $r \equiv 0$ (no compensation) the rotor is rotated and the X-Y plot of sensor output is shown in Figure 5. The vibration is believed to be caused by rotor imbalance. It is noted that all the data shown are down-sampled by a factor of 10, giving a data sample rate of 1000 Hz.

Test of Clean-Current Strategy

In this case the local feedback is disabled by letting $k = 0$. Stability of the compensation loop can be tested by observing its transient. At a constant speed of 1000 rpm and with initial values of $u_a = u_b = 0$, ε is switched from zero to normal, which gives rise to a transient in Figure 6. It takes about 10 seconds for the transient to become negligible. Figure 7 shows the steady-state X-Y plot of sensor output. Note that rotational center is dependent on rotational speed. Thus rotation about the mass center is not achieved by the clean-current strategy.

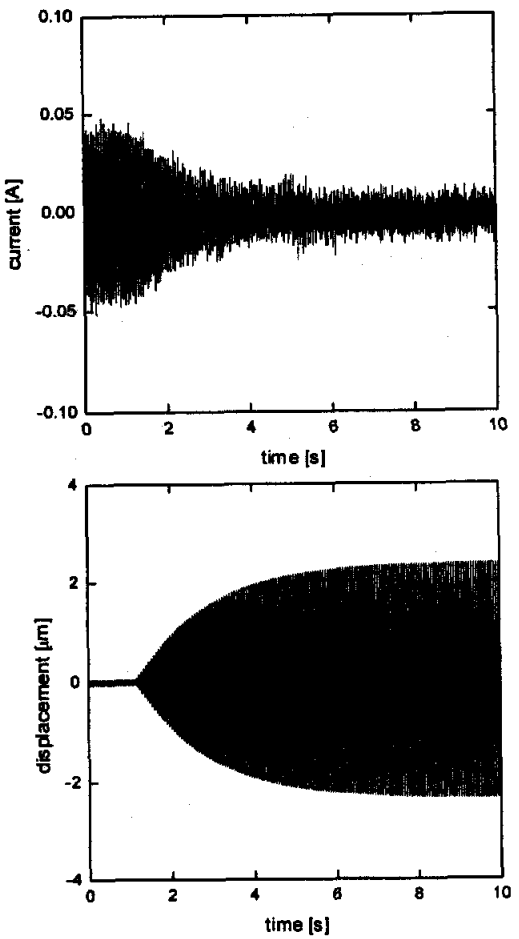

FIGURE 6: Transient of compensation loop.

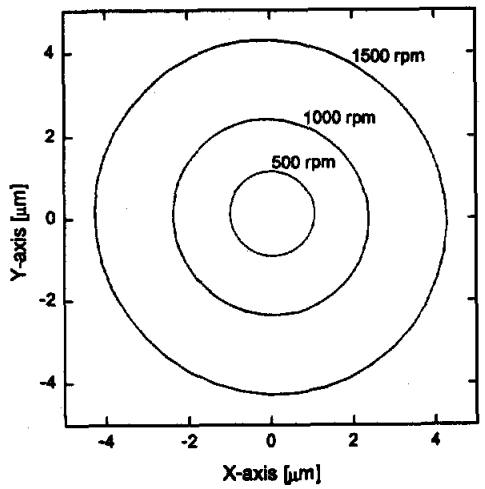

FIGURE 7: Steady-state X-Y plot with clean current.

Rotation about the Mass Center

With $k = 0$ the value of p/q is identified by letting $r \equiv r_p = +20$ μm and then $r \equiv r_n = -20$ μm, and finding the steady-state values of current i_p and i_n. As in steady state the force f in (2) must be zero, $-(i_p - i_n)/(r_p - r_n)$ gives an estimate of p/q. We obtain the values of 1.3929×10^4 (X) and 1.3704×10^4 (Y). Note that by the calculated p and q we have $p/q = 3.5\times10^5/23.6 = 1.48\times10^4$.

With k set to the estimates of p/q, the compensation loop is also stable, but it has a longer transient than the case of $k = 0$, because the local feedback alters the plant. Figure 8 shows the steady-state X-Y sensor output. Note that the amplitude is now not so strongly dependent on rotor speed. It is believed that at 1500 rpm the rotational center is close to the mass center, as checked below.

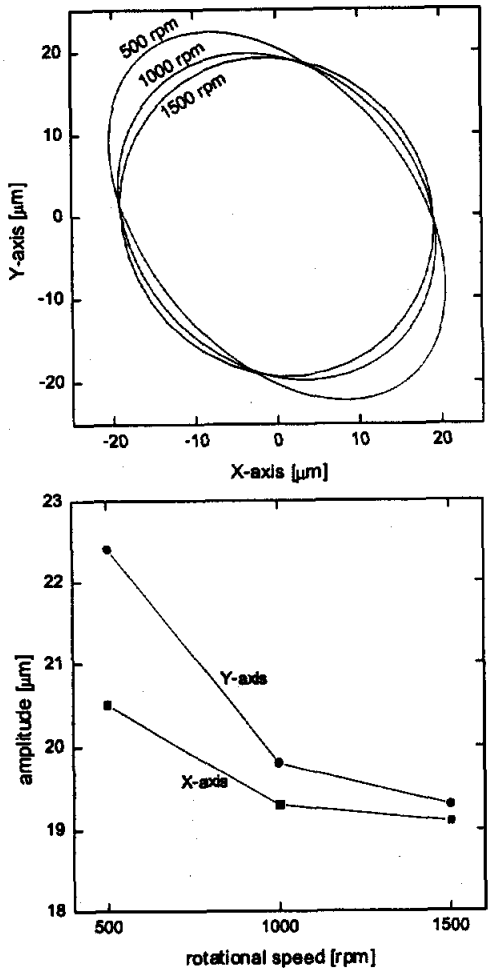

FIGURE 8: X-Y sensor output and its amplitude.

At 1500 rpm we switch ε to zero. At this moment the error signal e (see Figure 3 for meaning of e) must be free from the base harmonic. If we ignore the noise and higher harmonics we should have $e \equiv 0$ and $r \equiv x$, so the local feedback kx can be replaced by a feedforward term kr and (5) becomes

$$i = i_c - kr = C(s)(r - x) - kr \qquad (14)$$

Now the compensation is rendered open loop (since $\varepsilon = 0$), while e remains to be identically zero. The signal r is a function of only rotor angular position and defines a

rotational center about which the rotor is now rotating. Then we reduce the rotor speed. If the rotational center defined by r is not close to the mass center, we must expect to observe in e occurrences of vibrations as in Figure 5. The error e is plotted in Figure 9. Compared with Figure 5, in which case $r \equiv 0$ and rotation is about the geometric center, we see that the rotational center here as defined by r must be much closer to the mass center than the geometric center is.

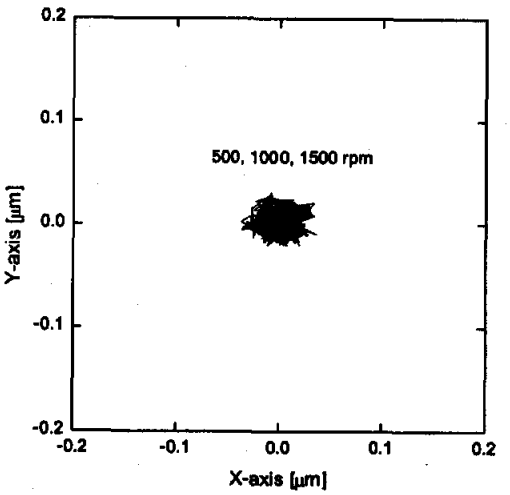

FIGURE 9: Error signal e at open-loop compensation.

CONCLUSIONS

Based on a planar rotor with a radial AMB, we have presented a simple method for removal of the vibration caused by rotor imbalance. Compared with the clean-current strategy, the given method is only slightly more complicated. It only additionally requires a local static feedback and the match of the feedback gain with the ratio of two plant parameters. As shown in experiment, this ratio is easily identified to such an accuracy that the local feedback gives significant improvement over plain clean-current strategy. The local feedback may give rise to a pair of zeros on the imaginary axis in the dynamics of the stabilizing loop, which prevents the compensation from working. This problem is easily avoided. What is more, this problem can be completely avoided after the mass center is located, since after that the compensation loop can be switched open, while rotation continues to be about the mass center for any rotational speed.

REFERENCES

1. T. Mizuno, A Unifying Point of View of Controllers for Active Magnetic Bearings, Proc. of the 7th Int. Symp. on Magnetic Bearings, ETH Zurich, Switzerland, Aug. 2000, pp. 263-268
2. H. Zhao, L. Zhao, and W. Jiang, Simulation and Experimental Research on Unbalance Vibration Control of AMB Systems, Proc. of the 7th Int. Symp. on Magnetic Bearings, ETH Zurich, Switzerland, Aug. 2000, pp. 573-578
3. K. Nonami, Q. Fan, and H. Ueyama, Unbalance Vibration Control of Magnetic Bearing Systems Using Adaptive Algorithm with Disturbance Frequency Estimation, JSME Int. J. Series C, vol. 41 no. 2, June 1998, pp. 220-226
4. H.-S. Na and Y. Park, An Adaptive Feedforward Controller for Rejection of Periodic Disturbances, J. Sound and Vibration, vol. 201, no. 4, April 1997, pp. 427-435
5. C. R. Knospe, S. J. Fedigan, R. W. Hope, and R. D. Williams, A Multitasking DSP Implementation of Adaptive Magnetic Bearing Control, IEEE Trans. Contr. Syst. Tech., vol. 5, no. 2, March 1997, pp. 230-238
6. R. Herzog, P. Buhler, C. Gahler, and R. Larsonneur, Unbalance Compensation Using Generalized Notch Filters in the Multivariable Feedback of Magnetic Bearings, IEEE Trans. Contr. Syst. Tech., vol. 4, no. 5, Sep. 1996, pp. 580-586
7. K.-Y. Lum, V. T. Coppola, and D. S. Bernstein, Adaptive Autocentering Control for an Active Magnetic Bearing Supporting a Rotor with Unknown Mass Imbalance, IEEE Trans. Contr. Syst. Tech., vol. 4, no. 5, Sep. 1996, pp. 587-597
8. A. M. Mohamed and I. Busch-Vishniac, Imbalance Compensation and Automation Balancing in Magnetic Bearing Systems Using the Q-Parameterization Theory, IEEE Trans. Contr. Syst. Tech., vol. 3, no. 2, June 1995, pp. 202-211
9. Y. Suzuki, S. Michimura, and A. Tamura, Unbalance Response Attenuation of a Flexible Rotor Suspended by Magnetic Bearings with Open Loop Control, JSME Int. J. Series C, vol. 37, no. 2, June 1994, pp. 285-291
10. B. Shafai, S. Beale, P. LaRocca, and E. Cusson, Magnetic Bearing Control Systems and Adaptive Forced Balancing, IEEE Contr. Syst. Mag., vol. 14, no. 2, April 1994, pp. 4-13
11. T. Higuchi, T. Mizuno, and M. Tsukamoto, Digital Control System for Magnetic Bearings with Automatic Balancing. Proc. of the 2nd Int. Symp. on Magnetic Bearings, Tokyo, Japan, July 12-14, 1990, pp. 27-32
12. L. Li, T. Shinshi, C. Iijima, X. Zhang, and A. Shimokohbe, Compensation of Rotor Imbalance for Precision Rotation of a Planar Magnetic Bearing Rotor, submitted to Precision Engineering